Journal of Statistical Physics, Vol. 81, Nos. 1/2, 1995

Analytical Solutions of the Lattice Boltzmann BGK Model

Qisu Zou,[1,2] Shuling Hou,[1,3] and Gary D. Doolen[1]

Received January 13, 1995

Analytical solutions of the two-dimensional triangular and square lattice Boltzmann BGK models have been obtained for the plane Poiseuille flow and the plane Couette flow. The analytical solutions are written in terms of the characteristic velocity of the flow, the single relaxation time τ, and the lattice spacing. The analytic solutions are the exact representation of these two flows without any approximation. Using the analytical solution, it is shown that in Poiseuille flow the bounce-back boundary condition introduces an error of first order in the lattice spacing. The boundary condition used by Kadanoff *et al.* in lattice gas automata to simulate Poiseuille flow is also considered for the triangular lattice Boltzmann BGK model. An analytical solution is obtained and used to show that the boundary condition introduces an error of second order in the lattice spacing.

KEY WORDS: Lattice Boltzmann methods; analytical solution; channel flow; Couette flow.

1. INTRODUCTION

Since the appearance of lattice gas automata (LGA) and its later derivative, the lattice Boltzmann equation method (LBE), as alternative computational methods to study transport phenomena, some analytical solutions have been obtained for these methods for nonuniform flows in 2D or 3D models.[3–6] They are based on linearized Boltzmann models, and

[1] Center for Nonlinear Studies and Theoretical Division, Los Alamos National Laboratory, Los Alamos, New Mexico 87545.
[2] Department of Mathematics, Kansas State University, Manhattan, Kansas 66506.
[3] Department of Mechanical Engineering, Kansas State University, Manhattan, Kansas 66506.

0022-4715/95/1000-0319$07.50/0

employ approximations. In refs. 3–5 the solution around a global equilibrium with constant density and isotropic velocity (zero velocity) was considered. In ref. 6 the first order and second order of deviation of the distribution function from equilibrium were assumed to take a certain form in terms of flow quantities, and the coefficients in this form were obtained using a Chapman–Enskog procedure. These analytic results provided insight for applications of the methods. For example, the analytical results allow one to calculate viscosity from given collision rules and to estimate and to improve bounce-back boundary conditions for LGA. They are valuable in enhancing our understanding of the method. Nevertheless, analytical solutions for real flows with boundaries like the Poiseuille flow, which is represented exactly by a second-order finite-difference scheme on a uniform mesh, have not been obtained previously for LGA or LBE. One reason may be that the boundary conditions used in LGA and LBE are not exact. For example, bounce-back or a combination of bounce-back and specular reflection[4] for modeling the nonslip boundary condition are only approximate. The effective nonslip boundary is inside the bounce-back row.[4, 6] Recently, Noble *et al.*[7] proposed a boundary condition for the lattice Boltzmann BGK model (LBGK) on a triangular lattice. When this boundary condition was applied to plane Poiseuille flow, the steady-state solution of the distribution function gave a parabolic velocity profile up to machine accuracy. The result suggests the existence of an analytical solution to LBGK, which is an exact representation of the Poiseuille flow. In this paper, analytical solutions for the Poiseuille flow are derived together with analytical solutions for the plane Couette flow for both triangular and square lattices.

2. ANALYTICAL SOLUTIONS OF THE TRIANGULAR LATTICE LBGK MODEL

First let us consider the lattice Boltzmann model on a triangular lattice (FHP model). For a channel flow, a triangular lattice is constructed as shown in Fig. 1. There are two types of particles on each node of an FHP model: rest particles (type 0) with $\mathbf{e}_0 = 0$ and moving particles (types 1–6) with unit velocity $\mathbf{e}_i = (\cos[(i-1)\pi/6],\ \sin[(i-1)\pi/6],\ i = 1,..., 6$, along six directions. Consider the particle distribution functions $f_i(\mathbf{x}, t)$, which represent the probability of finding a particle at node $\mathbf{x} = (x, y)$ and time t with velocity $\mathbf{e}_i$. The lattice Boltzmann BGK model proposed in refs. 8 and 9 is the eqution for the evolution of f_i:

$$f_i(\mathbf{x} + \delta\mathbf{e}_i, t + \delta) - f_i(\mathbf{x}, t) = -\frac{1}{\tau}[f_i(\mathbf{x}, t) - f_i^{(0)}(\mathbf{x}, t)], \qquad i = 0,..., 6 \quad (1)$$

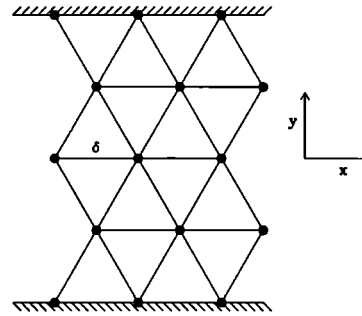

Fig. 1. The geometry of the plane channel flow.

where $f_i^{(0)}(\mathbf{x}, t)$ is the equilibrium distribution of the particle of type i at $\mathbf{x}$, t, the right-hand side represents the collision term, and τ is the single relaxation time which controls the rate of approach to equilibrium. The density per node, ρ, and the macroscopic flow velocity, $\mathbf{u}$, are defined in terms of the particle distribution function by

$$\sum_{i=0}^{6} f_i = \rho, \qquad \sum_{i=1}^{6} f_i \mathbf{e}_i = \rho \mathbf{u} \tag{2}$$

The equilibrium distribution functions depend only on local density and velocity. A suitable equilibrium distribution for the FHP model can be chosen in the following form[9]:

$$\begin{aligned} f_0^{(0)} &= d_0 - \rho \mathbf{u} \cdot \mathbf{u} = \alpha\rho - \rho \mathbf{u} \cdot \mathbf{u} \\ f_i^{(0)} &= d + \tfrac{1}{3}\rho[(\mathbf{e}_i \cdot \mathbf{u}) + 2(\mathbf{e}_i \cdot \mathbf{u})^2 - \tfrac{1}{2}\mathbf{u} \cdot \mathbf{u}], \qquad i = 1,\ldots, 6 \end{aligned} \tag{3}$$

where α is an adjustable parameter, $d = (\rho - d_0)/6$, and $\sum_i f_i^{(0)} = \rho$, $\sum_i f_i^{(0)} \mathbf{e}_i = \rho \mathbf{u}$. Note that Eq. (1) is written in physical units with the value of the lattice link being δ. Using unit speed for particles (with some physical time unit), a time step has the value of δ as well. A Chapman–Enskog procedure can be applied to Eq. (1) to derive the macroscopic equations of the model. They are given by: the continuity equation [with an error term $O(\delta^2)$ being omitted]

$$\frac{\partial \rho}{\partial t} + \nabla \cdot (\rho \mathbf{u}) = 0 \tag{4}$$

and the momentum equation [with terms $O(\delta^2)$ and $O(\delta u^3)$ being omitted]

$$\partial_t(\rho u_\alpha) + \partial_\beta(\rho u_\alpha u_\beta) = -\partial_\alpha(c_s^2 \rho) + \partial_\beta(2\nu\rho S_{\alpha\beta}) \tag{5}$$

where the Einstein summation convention is used, $S_{\alpha\beta}=\frac{1}{2}(\partial_\alpha u_\beta+\partial_\beta u_\alpha)$ is the strain-rate tensor, the pressure is given by $p=c_s^2\rho$, where c_s is the speed of sound with $c_s^2=(1-\alpha)/2$, and $\nu=[(2\tau-1)/8]\delta$, with ν the kinematic viscosity. The form of the error terms and the derivation of these equations can be found in refs. 10 and 11. The macroscopic equations of LBGK represent the incompressible Navier–Stokes equations in the limit as $\delta\to 0$, $\rho\to\rho_0$ (a constant) and the Mach number approaches zero.

The plane Poiseuille flow in a channel with $2L$ and velocity $\mathbf{u}=(u_x, u_y)$ is given by

$$u_x=u_0\left(1-\frac{y^2}{L^2}\right), \qquad u_y=0, \qquad \frac{\partial p}{\partial x}=-G, \qquad \frac{\partial p}{\partial y}=0 \tag{6}$$

where G is a constant related to the characteristic velocity u_0 by

$$G=2\rho\nu u_0/L^2 \tag{7}$$

and the flow density ρ is a constant. This is an exact solution of the incompressible Navier–Stokes equations:

$$\begin{gathered}\nabla\cdot\mathbf{u}=0\\ \partial_t(\rho u_\alpha)+\partial_\beta(\rho u_\alpha u_\beta)=-\partial_\alpha p+\mu\partial_{\beta\beta}u_\alpha\end{gathered} \tag{8}$$

where $\mu=\rho\nu$. Without loss of generality, we assume that $L=1$ (a simple scaling of $y'=y/L$ makes $y'\in[-1, 1]$). To approximate Poiseuille flow using the lattice Boltzmann model, it is convenient to replace the constant gradient by a body force $\mathbf{g}$ so that $\rho\mathbf{g}=-\nabla p$. The momentum equation of NS equations with a body force is

$$\partial_t(\rho u_\alpha)+\partial_\beta(\rho u_\alpha u_\beta)=-\partial_\alpha p+\rho g_\alpha+\mu\partial_{\beta\beta}u_\alpha \tag{9}$$

The Poiseuille flow can be generated with a body foce $\mathbf{g}$ with $\rho g_x=G$, $g_y=0$, where the pressure is held constant. An LBGK which incorporates the body force is a modification of Eq. (1) given by

$$f_i(\mathbf{x}+\delta\mathbf{e}_i, t+\delta)-f_i(\mathbf{x}, t)=-\frac{1}{\tau}[f_i(\mathbf{x}, t)-f_i^{(0)}(\mathbf{x}, t)]+\delta h_i \tag{10}$$

where the h_i are chosen as

$$h_0=0, \quad h_i=+G/4, \quad i=1, 2, 6; \qquad h_i=-G/4, \quad i=3, 4, 5 \tag{11}$$

so that

$$\sum_i h_i=0, \qquad \sum_i h_i\mathbf{e}_i=\rho\mathbf{g}, \qquad \sum_i h_i e_{i\alpha}e_{i\beta}=0$$

Now suppose there exists a solution $f_i(\mathbf{x}, t)$ of Eq. (10) and it exactly represents the Poiseuille flow. We then expect the following properties:

1. $f_i(\mathbf{x}, t)$ is steady (independent of t).
2. $f_i(\mathbf{x}, t)$ is independent of x, hence is only a function of y, denoted by $f_i(y)$.
3. $f_2(y) = f_6(-y)$, and $f_3(y) = f_5(-y)$ from the symmetry of the flow.
4. $\sum_i f_i(y) = \rho$ (constant).
5. $\sum_i f_i(y)\, e_{ix} = \rho u_x(y)$, where $u_x(y) = u_0(1 - y^2)$ (remember $L = 1$).
6. $\sum_i f_i(y)\, e_{iy} = 0$.

According to Eq. (3), the equilibrium distributions are given by

$$
\begin{aligned}
&f_0^{(0)} = d_0 - \rho u^2 \qquad [u = u_x(y)] \\
&f_1^{(0)} = d + \frac{\rho}{3} u + \frac{\rho}{2} u^2, \qquad && f_4^{(0)} = d - \frac{\rho}{3} u + \frac{\rho}{2} u^2 \\
&f_2^{(0)} = d + \frac{\rho}{6} u, && f_3^{(0)} = d - \frac{\rho}{6} u \\
&f_5^{(0)} = d - \frac{\rho}{6} u, && f_6^{(0)} = d + \frac{\rho}{6} u
\end{aligned}
\tag{12}
$$

$d = (\rho - d_0)/6$. Using properties 1 and 2 and Eq. (10) for $i = 0$ gives

$$f_0(y) = f_0(y) - \frac{1}{\tau}\left(f_0(y) - f_0^{(0)}(y)\right)$$

Hence

$$f_0(y) = f_0^{(0)}(y) = d_0 - \rho u^2 \tag{13}$$

Equation (10) for $i = 1$ gives

$$f_1(y) = f_1(y) - \frac{1}{\tau}\left(f_1(y) - f_1^{(0)}(y)\right) + \delta \frac{G}{4}$$

Hence

$$f_1(y) = f_1^{(0)}(y) + \tau \delta G/4 \tag{14}$$

Similarly

$$f_4(y) = f_4^{(0)}(y) - \tau \delta G/4 \tag{15}$$

It is seen that f_0, f_1, f_4 are functions of y^4, y^2 through dependence of u and u^2. To find the remaining $f_i(y)$, we note that $f_i^{(0)}$, $i=2, 3, 5, 6$, do not have a u^2 term and thus are functions of y^2 only, so the following form is suggested:

$$f_i(y) = a_i + b_i y + c_i y^2, \qquad i=2, 3, 5, 6 \tag{16}$$

where the 12 unknown coefficients a_i, b_i, c_i depend on flow quantities τ and dy, but not on y. Using property 3, we obtain

$$a_2 + b_2 y + c_2 y^2 = a_6 - b_6 y + c_6 y^2, \qquad a_3 + b_3 y + c_3 y^2 = a_5 - b_5 y + c_5 y^2$$

which should be true for any y; thus

$$a_6 = a_2, \qquad b_6 = -b_2, \qquad c_6 = c_2$$
$$a_5 = a_3, \qquad b_5 = -b_3, \qquad c_5 = c_3$$

Similarly, using property 6, we find

$$2b_2 y + 2b_3 y = 0, \qquad \text{hence} \quad b_3 = -b_2 \tag{18}$$

Property 4 with information obtained gives

$$2(a_2 + a_3) + 2(c_2 + c_3) y^2 + f_0(y) + f_1(y) + f_4(y) = \rho \tag{19}$$

On using the expressions for f_0, f_1, f_4 given in Eqs. (13)–(15), we find (on using the expression of d)

$$a_2 + a_3 = \tfrac{1}{2}(\rho - d_0 - 2d) = 2d \tag{20a}$$

and

$$c_3 + c_2 = 0 \tag{20b}$$

which gives

$$c_3 = -c_2, \qquad a_3 = 2d - a_2 \tag{21}$$

Similarly, property 5 with information obtained yields

$$a_2 = \frac{1}{6}\rho u_0 + d - \frac{\tau \delta G}{4}; \qquad c_2 = -\frac{1}{6}\rho u_0 \tag{22}$$

At this point, only b_2 remains unknown. Using Eq. (10) for $i=2$, we have

$$f_2(y + dy) = f_2(y) - \frac{1}{\tau}(f_2(y) - f_2^{(0)}(y)) + \frac{\delta G}{4} \tag{23}$$

where dy is the vertical spacing between two lattice rows and $dy = (\sqrt{3}/2)\delta$. On using the expression for $f_2^{(0)}$, we can obtain

$$c_2[y^2 + 2y\,dy + (dy)^2] + b_2 y + b_2\,dy + a_2$$
$$= \left(1 - \frac{1}{\tau}\right)(c_2 y^2 + b_2 y + a_2) + \frac{1}{\tau}\left[d + \frac{1}{6}\rho u_0(1 - y^2)\right] + \frac{\delta G}{4} \quad (24)$$

The balance of terms linear in y yields

$$b_2 = -2\tau c_2\,dy = \tfrac{1}{3}\tau\rho u_0\,dy \quad (25)$$

and fortunately the equations for the coefficients of y^2 and y^0 are both satisfied. It is easy to check that the evolution equations for f_3, f_5, f_6 are all satisfied with the choice of a_i, b_i, c_i obtained so far.

Putting these results all together, we find that the quantities

$$f_0 = d_0 - \rho u^2$$

$$f_1 = d + \frac{\rho}{3}u + \frac{\rho}{2}u^2 + \frac{\tau\delta G}{4}$$

$$f_4 = d - \frac{\rho}{3}u + \frac{\rho}{2}u^2 - \frac{\tau\delta G}{4}$$

$$f_2 = -\frac{1}{6}\rho u_0 y^2 + \frac{1}{3}\tau\rho u_0 y\,dy + \frac{1}{6}\rho u_0 + d - \frac{\tau\delta G}{4} \quad (26)$$

$$f_3 = +\frac{1}{6}\rho u_0 y^2 - \frac{1}{3}\tau\rho u_0 y\,dy - \frac{1}{6}\rho u_0 + d + \frac{\tau\delta G}{4}$$

$$f_5 = +\frac{1}{6}\rho u_0 y^2 + \frac{1}{3}\tau\rho u_0 y\,dy - \frac{1}{6}\rho u_0 + d + \frac{\tau\delta G}{4}$$

$$f_6 = -\frac{1}{6}\rho u_0 y^2 - \frac{1}{3}\tau\rho u_0 y\,dy + \frac{1}{6}\rho u_0 + d - \frac{\tau\delta G}{4}$$

satisfy properties 1–6 and that they together with the equilibrium distribution given in Eq. (12) satisfy the LBGK equation, Eq. (10). Hence it is an exact representation of the Poiseuille flow in the region $y \in [-1, 1]$.

Next, let us see to what boundary condition the solution in Eq. (26) corresponds. Taking the bottom boundary with $y = -1$, $u = 0$, we have

$$f_0 = d_0, \qquad f_1 = d + \frac{\tau\delta G}{4}, \qquad f_4 = d - \frac{\tau\delta G}{4}$$

$$f_2 = -\frac{1}{3}\tau\rho u_0\, dy + d - \frac{\tau\delta G}{4}, \qquad f_3 = +\frac{1}{3}\tau\rho u_0\, dy + d + \frac{\tau\delta G}{4} \tag{27}$$

$$f_5 = -\frac{1}{3}\tau\rho u_0\, dy + d + \frac{\tau\delta G}{4}, \qquad f_6 = +\frac{1}{3}\tau\rho u_0\, dy + d - \frac{\tau\delta G}{4}$$

It is seen that on the bottom, after the collision and forcing, $f_2 = f_5 - 2\tau\delta G/4$, $f_3 = f_6 + 2\tau\delta G/4$. Hence, if a bounce-back boundary condition $f_2 = f_5$, $f_3 = f_6$ on f_2, f_3 is applied at the bottom to replace the collision and forcing step, the error is of order δ. This shows that the bounce-back boundary condition is first-order accurate. This has been confirmed in computations.[11-13]

To obtain the steady-state analytical solution in the LBGK simulations, the boundary condition should be suitably chosen for the simulation. The boundary condition proposed by Nobel *et al.*[7] is a suitable choice. If we are looking at a node B on the bottom, after streaming, f_2 and f_3 are empty at the node B, since no particle is coming from outside. Then Eqs. (2) with $u_x = u_y = 0$ are used to determine ρ, f_2, f_3. Then the normal collision with force as given in Eq. (10) is applied to f_i on the boundaries. Suppose that initially we use uniform density ρ_0 and zero velocity through the flow field; then we compute $f_i^{(0)}(0)$ and set $f_i = f_i^{(0)}$ through the field. Since there are no pressure gradients, it is natural that the density at each node remains constant ρ_0 (confirmed by simulations). Therefore Eqs (2) can be used to find the unique f_2, f_3 with the correct density and velocity, hence they are consistent with the evoluation of f_2, f_3 in the analytical solution. Simulation results indicate that the numerical solution with this boundary condition approaches the analytical solution as $t \to \infty$.

It is noted that the solution given in Eq. (26) satisfies the LBGK equation, Eq. (10), for any y and it gives an x velocity of $u_0(1-y^2)$. In the region $y \in [-1, 1]$ it represents the Poiseuille flow. The flow can be extended beyond the region $y \in [-1, 1]$ with the given parabolic velocity profile $u_0(1-y^2)$. In the work by Kadanoff *et al.*[1,2] a special treatment of the problem (square wave forcing) is employed for the LGA method to simulate Poiseuille flow. The simulation region is doubled in the y direction, with uniform forcing in the positive x direction for $-1 \leqslant y < 1$ (the lower channel, assuming the width of the channel is 2) and uniform forcing in the negative x direction for $1 \leqslant y \leqslant 3$ (the upper channel). Periodic boundary conditions on both the x and y directions are used. The solution in lower or upper channel represents Poiseuille flow. Figure 2 gives an

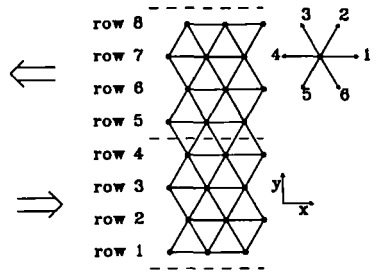

Fig. 2. Square wave forcing for the plane channel flow. Dashed lines indicate the positions of walls. The two large arrows indicate the directions of uniform forcing.

example of the configuration. In the figure, dashed lines indicate the positions of walls; the number of rows in each channel is four, but it can be an odd number also. This treatment avoids the use of the bounce-back boundary condition and it produces better results. It is interesting to consider this treatment for the LBGK equation, Eq. (10). Simulations in refs 1 and 2 suggest that the steady-state velocity profile in each channel is parabolic. First, let us check whether the analytical solution given in Eq. (26) is a solution of this problem. We consider the lower channel of width 2 with the coordinate system as shown in Fig. 2 so that the origin is at the center of the channel. Obviously from the derivation of the solution in Eq. (26), if $\mathbf{x}$, $\mathbf{x}+\mathbf{e}_i$ are inside the channel, then the solution in Eq. (26) satisfies Eq. (10) with $\rho = \text{const}$, $\mathbf{u} = (u_0(1-y^2), 0)$. The real problem occurs when Eq. (10) involves nodes on both lower and upper channels. For example, consider the case where $i=2$, $\mathbf{x}$ is a node on row 4 with y coordinate $y_4 = 1 - \frac{1}{2}dy$; and nodes on row 5 have y coordinate $y_5 = 1 + \frac{1}{2}dy$ as shown in Fig. 2. In this case, Eq. (10) becomes

$$f_2(y_5) = f_2(y_4) - \frac{1}{\tau}(f_2(y_4) - f_2^{(0)}(y_4)) + \frac{\delta G}{4} \tag{28}$$

Since the upper channel has the opposite parabolic velocity profile, $f_2(y_5) = f_5(y_4)$. Hence,

$$f_5(y_4) = f_2(y_4) - \frac{1}{\tau}(f_2(y_4) - f_2^{(0)}(y_4)) + \frac{\delta G}{4} \tag{29}$$

Substituting $f_2(y_4)$, $f_2^{(0)}(y_4)$, $f_5(y_4)$ in Eqs. (12) and (26) into Eq. (29) gives

$$\tfrac{1}{16}\rho u_0 \delta^2(4\tau^2 - 7\tau + 1) = 0 \tag{30}$$

Hence the solution in Eq. (26) does not satisfy Eq. (10) unless $4\tau^2 - 6\tau + 1 = 0$, which gives two roots of $\tau_+ = (3+\sqrt{5})/4 \approx 1.3090$, $\tau_- = (3-\sqrt{5})/4 \approx 0.3820$.

Next let us look for an exact solution of Eq. (10) for the configuration shown in Fig. 2. We consider the lower channel with forcing G given by Eq. (7). We know that the velocity profile is slightly different from the exact Poiseuille velocity profile. Nevertheless, we still expect the six properties mentioned before Eq. (12) with the x velocity $u_x(y) = u_0(1-y^2)$ being replaced by

$$u_x(y) = \bar{u}_0(1 + k - y^2) \qquad \text{for some constants } \bar{u}_0, k \tag{31}$$

so that the velocity profile is still symmetric about the centerline of the channel. When Eq. (10) involves nodes on both lower and upper channels, we use an equation like Eq. (29). The equilibrium distribution is still given by Eq. (12). It is easy to see that f_0, f_1, f_4 are still given by Eqs. (13)–(15) with $u = u_x(y)$ given in Eq. (31). Then assuming $f_i(y) = a_i + b_i y + c_i y^2$, $i = 2, 3, 5, 6$, and using properties 1–6 and Eq. (10) inside the lower channel, it is found that

$$\bar{u}_0 = u_0$$

[u_0 is related to the forcing by Eq. (7)], and

$$\begin{aligned} a_2 &= a_6 = \frac{1}{6}\rho u_0(1+k) + d - \frac{\tau \delta G}{4} \\ a_3 &= a_5 = -\frac{1}{6}\rho u_0(1+k) + d + \frac{\tau \delta G}{4} \\ b_2 &= -b_6 = -b_3 = b_5 = \frac{1}{3}\tau \rho u_0\, dy \\ c_2 &= c_6 = -c_3 = -c_5 = -\frac{1}{6}\rho u_0 \end{aligned} \tag{32}$$

Now only k is undetermined. Applying Eq. (10) for $i = 2$ across the wall between lower and upper channels gives

$$f_5(y_-) = f_2(y_-) - \frac{1}{\tau}(f_2(y_-) - f_2^{(0)}(y_-)) + \frac{\delta G}{4} \tag{33}$$

where $y_- = 1 - \frac{1}{2}dy$ is the y coordinate of the row just below the wall. Solving this equation gives

$$k = \tfrac{3}{16}(4\tau^2 - 6\tau + 1)\,\delta^2$$

It is easy to check that Eq. (10) is satisfied for other i's across the wall. Hence an exact solutions of Eq. (10) in the lower channel in this case is given by

$$
\begin{aligned}
f_0 &= d_0 - \rho u^2 \\
f_1 &= d + \frac{\rho}{3} u + \frac{\rho}{2} u^2 + \frac{\tau \delta G}{4} \\
f_4 &= d - \frac{\rho}{3} u + \frac{\rho}{2} u^2 - \frac{\tau \delta G}{4} \\
f_2 &= -\frac{1}{6} \rho u_0 y^2 + \frac{1}{3} \tau \rho u_0 y \, dy + \frac{1}{6} \rho u_0 (1+k) + d - \frac{\tau \delta G}{4} \\
f_3 &= +\frac{1}{6} \rho u_0 y^2 + \frac{1}{3} \tau \rho u_0 y \, dy - \frac{1}{6} \rho u_0 (1+k) + d + \frac{\tau \delta G}{4} \\
f_5 &= +\frac{1}{6} \rho u_0 y^2 + \frac{1}{3} \tau \rho u_0 y \, dy - \frac{1}{6} \rho u_0 (1+k) + d + \frac{\tau \delta G}{4} \\
f_6 &= -\frac{1}{6} \rho u_0 y^2 - \frac{1}{3} \tau \rho u_0 y \, dy + \frac{1}{6} \rho u_0 (1+k) + d - \frac{\tau \delta G}{4}
\end{aligned}
\tag{35}
$$

with $u = u_x(y) = u_0(1 + k - y^2)$ and k is given by Eq. (34). The solution in the upper channel can be obtained by antisymmetry about the wall. In the lower or upper channel, the steady-state solution of Eq. (10) gives a discrete representation of an exact parabolic x-velocity profile with the maximum velocity given by $u_0(1+k)$. The relative error in the maximum velocity is k, which is $O(\delta^2)$. The parabolic profile has a value of $u_0 k$ at the wall ($y = -1$ or $y = 1$). The nonzero value of the velocity at the wall is also $O(\delta^2)$, indicating second-order accuracy. When $\tau = \tau_+ = (3 + \sqrt{5})/4 \approx 1.3090$, $k = 0$, the simulation gives the exact Poiseuille flow corresponding to the forcing. $\tau_- = (3 - \sqrt{5})/4$ also makes $k = 0$, but the simulation is unstable for this value of τ. It also noted that for a fixed lattice size (fixed δ), if $\tau \to \infty$, then the error also goes to infinity. These conclusions are confirmed by numerical simulations.

Next, let us consider a plane Couette flow, where the flow between two parallel plates (corresponding to $y = 0$ and $y = 1$) is driven by the constantly moving top plate with velocity u_0. In this case, the solution is given by

$$
u = u_x = u_0 y, \qquad 0 \leqslant y < 1, \qquad u_y = 0, \qquad \nabla p = 0 \tag{36}
$$

with ρ a constant and with no body force. So the LBGK model, Eq. (1), is used. Using a similar procedure, we find the analytical solution of Eq. (1) representing the Couette flow:

$$f_0 = d_0 - \rho u^2, \qquad f_1 = d + \frac{\rho}{3}u + \frac{\rho}{2}u^2, \qquad f_4 = d - \frac{\rho}{3}u + \frac{\rho}{2}u^2$$

$$f_2 = +\frac{1}{6}\rho u_0 y + d - \frac{1}{6}\tau\rho u_0\, dy, \qquad f_3 = -\frac{1}{6}\rho u_0 y + d + \frac{1}{6}\tau\rho u_0\, dy \quad (37)$$

$$f_5 = -\frac{1}{6}\rho u_0 y + d - \frac{1}{6}\tau\rho u_0\, dy, \qquad f_6 = +\frac{1}{6}\rho u_0 y + d + \frac{1}{6}\tau\rho u_0\, dy$$

We note that these analytical solutions are valid for any u_0, τ, and dy.

3. ANALYTICAL SOLUTIONS OF THE SQUARE LATTICE LBGK MODEL

The square lattice Boltzmann BGK model is proven to be more robust than the triangular model in numerical simulations.[11, 14] It is important and interesting to find analytical solutions for it. The square lattice Boltzmann BGK model uses three types of particles. Particles of type 1 move along the x axis or the y axis with speed $\mathbf{e}_i = (\cos[\pi(i-1)/2], \sin[\pi(i-1]/2)$, $i = 1, 2, 3, 4$, and particle of type 2 move along the diagonal directions with speed $\mathbf{e}_i = \sqrt{2}(\cos[\pi(i-4-\frac{1}{2})/2], \sin[\pi(i-4-\frac{1}{2})/2]$, $i = 5, 6, 7, 8$. Rest particles of type 0 with $\mathbf{e}_0 = 0$ (speed zero) are also allowed at each node. Each node is connected to its 8 nearest neighbors by 8 links of length δ (in physical units) or $\sqrt{2}\,\delta$ as shown in Fig. 3. The single-particle distribution function $f_i(\mathbf{x}, t)$ again satisfies the LBGK model, Eq. (1) (with $i = 0, \ldots, 8$). The density ρ and the macroscopic velocity $\mathbf{u}$ are still defined in Eq. (2). For the square lattice, the equilibrium distribution can be chosen in the following form for particles of each type (the model d2q9[9]):

$$\begin{aligned} f_0^{(0)} &= \tfrac{4}{9}\rho[1 - \tfrac{3}{2}\mathbf{u}\cdot\mathbf{u}] \\ f_i^{(0)} &= \tfrac{1}{9}\rho[1 + 3(\mathbf{e}_i\cdot\mathbf{u}) + \tfrac{9}{2}(\mathbf{e}_i\cdot\mathbf{u})^2 - \tfrac{3}{2}\mathbf{u}\cdot\mathbf{u}], \qquad i = 1, 2, 3, 4 \\ f_i^{(0)} &= \tfrac{1}{36}\rho[1 + 3(\mathbf{e}_i\cdot\mathbf{u}) + \tfrac{9}{2}(\mathbf{e}_i\cdot\mathbf{u})^2 - \tfrac{3}{2}\mathbf{u}\cdot\mathbf{u}], \qquad i = 5, 6, 7, 8 \end{aligned} \quad (38)$$

with

$$\sum_\sigma \sum_i f_{\sigma i}^{(0)} = \rho, \qquad \sum_\sigma \sum_i f_{\sigma i}^{(0)} \mathbf{e}_{\sigma i} = \rho\mathbf{u}$$

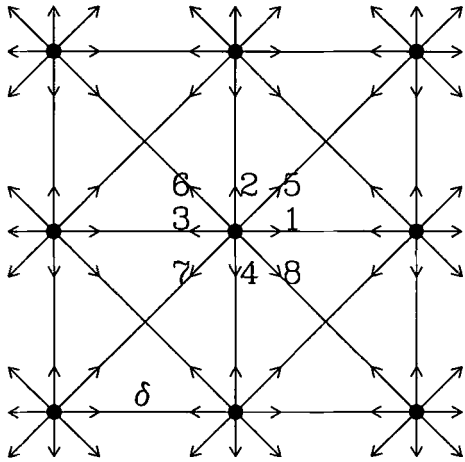

Fig. 3. A square lattice.

The macroscopic equations of the model are the same as given in Eqs. (4) and (5) with $c_s^2 = 1/3$, and $v = [(2\tau - 1)/6]\delta$. To incorporate a body foce into model Poiseuille flow, Eq. (10) ($i = 0,..., 8$) is used, with h_i being chosen in the following way[15]

$$h_0 = 0, \quad h_1 = \tfrac{1}{3}G, \quad h_2 = 0, \quad h_3 = -\tfrac{1}{3}G, \quad h_4 = 0$$
$$h_5 = h_8 = \tfrac{1}{12}G, \quad h_6 = h_7 = -\tfrac{1}{12}G \tag{39}$$

To derive an analytical solution of Eq. (10) for the square lattice, we note that the six properties in Section 2 still apply, except that property 3 is replaced by:

3. $f_2(y) = f_4(-y)$, $f_5(y) = f_8(-y)$, and $f_6(y) = f_7(-y)$ from the symmetry of the flow.

Using a similar procedure as in Section 2, we can find that

$$f_0(y) = f_0^{(0)}(y) = \tfrac{4}{9}\rho(1 - \tfrac{3}{2}u^2) \qquad [u = u_0(1 - y^2)] \tag{40}$$

$$f_1(y) = \tfrac{1}{9}\rho(1 + 3u + 3u^2) + \tfrac{2}{3}\tau v \rho u_0 \delta \tag{41}$$

$$f_3(y) = \tfrac{1}{9}\rho(1 - 3u + 3u^2) - \tfrac{2}{3}\tau v \rho u_0 \delta \tag{42}$$

and

$$f_i(y) = a_i + b_i y + c_i y^2 + d_i y^3 + e_i y^4, \qquad i = 2, 4, 5, 6, 7, 8 \tag{43}$$

with

$$a_4=a_2,\quad b_4=-b_2,\quad c_4=c_2,\quad d_4=-d_2,\quad e_4=e_2$$
$$a_8=a_5,\quad b_8=-b_5,\quad c_8=c_5,\quad d_8=-d_5,\quad e_8=e_5$$
$$a_7=a_6,\quad b_7=-b_6,\quad c_7=c_6,\quad d_7=-d_6,\quad e_7=e_6$$

and

$$\begin{aligned}
a_2 &= -4\tau^4\rho u_0^2\delta^4+6\tau^3\rho u_0^2\delta^4-\tfrac{7}{3}\tau^2\rho u_0^2\delta^4+\tfrac{2}{3}\tau^2\rho u_0^2\delta^2\\
&\quad+\tfrac{1}{6}\tau\rho u_0^2\delta^4-\tfrac{1}{3}\tau\rho u_0^2\delta^2+\tfrac{1}{9}\rho-\tfrac{1}{6}\rho u_0^2\\
b_2 &= 4\tau^3\rho u_0^2\delta^3-4\tau^2\rho u_0^2\delta^3+\tfrac{2}{3}\tau\rho u_0^2\delta^3-\tfrac{2}{3}\tau\rho u_0^2\delta\\
c_2 &= -2\tau^2\rho u_0^2\delta^2+\tau\rho u_0^2\delta^2+\tfrac{1}{3}\rho u_0^2\\
d_2 &= \tfrac{2}{3}\tau\rho u_0^2\delta\\
e_2 &= -\tfrac{1}{6}\rho u_0^2
\end{aligned}\tag{45}$$

$$\begin{aligned}
a_5 &= 2\tau^4\rho u_0^2\delta^4-3\tau^3\rho u_0^2\delta^4+\tfrac{7}{6}\tau^2\rho u_0^2\delta^4-\tfrac{1}{3}\tau^2\rho u_0^2\delta^2-\tfrac{1}{6}\tau^2\rho u_0\delta^2-\tfrac{1}{12}\tau\rho u_0^2\delta^4\\
&\quad+\tfrac{1}{6}\tau\rho u_0^2\delta^2+\tfrac{1}{12}\tau\rho u_0\delta^2+\tfrac{1}{36}\rho+\tfrac{1}{12}\rho u_0^2+\tfrac{1}{12}\rho u_0+\tfrac{1}{6}\tau^2\rho u_0\delta\\
b_5 &= -2\tau^3\rho u_0^2\delta^3+2\tau^2\rho u_0^2\delta^3-\tfrac{1}{3}\tau\rho u_0^2\delta^3+\tfrac{1}{3}\tau\rho u_0^2\delta+\tfrac{1}{6}\tau\rho u_0\delta\\
c_5 &= \tau^2\rho u_0^2\delta^2-\tfrac{1}{2}\tau\rho u_0^2\delta^2-\tfrac{1}{6}\rho u_0^2-\tfrac{1}{12}\rho u_0\\
d_5 &= -\tfrac{1}{3}\tau\rho u_0^2\delta\\
e_5 &= \tfrac{1}{12}\rho u_0^2
\end{aligned}\tag{46}$$

and

$$\begin{aligned}
a_6 &= 2\tau^4\rho u_0^2\delta^4-3\tau^3\rho u_0^2\delta^4+\tfrac{7}{6}\tau^2\rho u_0^2\delta^4-\tfrac{1}{3}\tau^2\rho u_0^2\delta^2+\tfrac{1}{6}\tau^2\rho u_0\delta^2-\tfrac{1}{12}\tau\rho u_0^2\delta^4\\
&\quad+\tfrac{1}{6}\tau\rho u_0^2\delta^2-\tfrac{1}{12}\tau\rho u_0\delta^2+\tfrac{1}{36}\rho+\tfrac{1}{12}\rho u_0^2-\tfrac{1}{12}\rho u_0-\tfrac{1}{6}\tau^2\rho u_0\delta\\
b_6 &= -2\tau^3\rho u_0^2\delta^3+2\tau^2\rho u_0^2\delta^3-\tfrac{1}{3}\tau\rho u_0^2\delta^3+\tfrac{1}{3}\tau\rho u_0^2\delta-\tfrac{1}{6}\tau\rho u_0\delta\\
c_6 &= \tau^2\rho u_0^2\delta^2-\tfrac{1}{2}\tau\rho u_0^2\delta^2-\tfrac{1}{6}\rho u_0^2+\tfrac{1}{12}\rho u_0\\
d_6 &= -\tfrac{1}{3}\tau\rho u_0^2\delta\\
e_6 &= \tfrac{1}{12}\rho u_0^2
\end{aligned}\tag{47}$$

Equations (40)–(42) together with Eqs. (43)–(47) completely specify the analytical solution, which is a solution of Eq. (10) and it exactly represents the Poiseuille flow.

Next, let us see to what boundary condition this analytical solution corresponds. Taking the bottom boundary with $y=-1$, $u=0$, we find the relation of $f_{\sigma i}$ after the collision and forcing:

$$f_1 - f_3 = \tfrac{4}{3}\tau v \rho u_0 \delta, \qquad f_2 - f_4 = -2\delta^3(4\tau^3 \rho u_0^2 - 4\tau^2 \rho u_0^2 + \tfrac{2}{3}\tau \rho u_0^2)$$
$$f_5 - f_7 = -\tfrac{2}{9}\tau^2 \rho u_0 \delta^2 + \tfrac{1}{9}\tau \rho u_0^2 \delta^2 + 4\tau^3 \rho u_0^2 \delta^3 - 4\tau^2 \rho u_0^2 \delta^3 + \tfrac{2}{3}\tau \rho u_0^2 \delta^3 \quad (48)$$
$$f_6 - f_8 = +\tfrac{2}{9}\tau^2 \rho u_0 \delta^2 - \tfrac{1}{9}\tau \rho u_0^2 \delta^2 + 4\tau^3 \rho u_0^2 \delta^3 - 4\tau^2 \rho u_0^2 \delta^3 + \tfrac{2}{3}\tau \rho u_0^2 \delta^3$$

If a bounce-back boundary condition in which f_1 exchanges with f_3, $f_2 = f_4$, $f_5 = f_7$, $f_6 = f_8$, is applied at the bottom to replace the collision and forcing step, the error introduced into f_1 and f_3 is of order δ. This shows that the bounce-back boundary condition is first-order accurate. This has been confirmed in computations.[11–13] To obtain the steady-state analytical solution derived in this paper in LBGK simulations, the boundary condition should be suitably chosen. No numerical simulation on a square lattice Boltzmann BGK model has obtained an exact solution for the Poiseuille flow so far. Of course, using $\tau = 1$ and providing the equilibrium distribution from zero velocity at the boundary is consistent with the analytical solution and gives the exact solution (confirmed in simulations), but $\tau = 1$ is too restrictive. If we provide the analytical solution on the boundary, we will be able to obtain the analytical solution in this region also (confirmed in simulations). Specification of the analytical solution on the boundary does not provide a boundary condition of general purpose. Nevertheless, the analytical solution will give some guidance in developing better boundary conditions of general purpose for the model.

The analytical solution solution for plane Couette flow is given by

$$f_0 = \tfrac{4}{9}\rho(1 - \tfrac{3}{2}u_0^2 y^2)$$
$$f_1 = \tfrac{1}{9}\rho(1 + 3u_0 y + 3u_0^2 y^2)$$
$$f_3 = \tfrac{1}{9}\rho(1 - 3u_0 y + 3u_0^2 y^2)$$
$$f_2 = -\tfrac{1}{3}\tau^2 \rho u_0^2 \delta^2 + \tfrac{1}{6}\tau \rho u_0^2 \delta^2 + \tfrac{1}{9}\rho + \tfrac{1}{3}\tau \rho u_0^2 \delta y - \tfrac{1}{6}\rho u_0^2 y^2$$
$$f_4 = -\tfrac{1}{3}\tau^2 \rho u_0^2 \delta^2 + \tfrac{1}{6}\tau \rho u_0^2 \delta^2 + \tfrac{1}{9}\rho - \tfrac{1}{3}\tau \rho u_0^2 \delta y - \tfrac{1}{6}\rho u_0^2 y^2$$
$$f_5 = \tfrac{1}{6}\tau^2 \rho u_0^2 \delta^2 - \tfrac{1}{12}\tau \rho u_0^2 \delta^2 - \tfrac{1}{12}\tau \rho u_0 \delta + \tfrac{1}{36}\rho$$
$$+ (-\tfrac{1}{6}\tau \rho u_0^2 \delta + \tfrac{1}{12}\rho u_0) y + \tfrac{1}{12}\rho u_0^2 y^2 \quad (49)$$
$$f_6 = \tfrac{1}{6}\tau^2 \rho u_0^2 \delta^2 - \tfrac{1}{12}\tau \rho u_0^2 \delta^2 + \tfrac{1}{12}\tau \rho u_0 \delta + \tfrac{1}{36}\rho$$
$$+ (-\tfrac{1}{6}\tau \rho u_0^2 \delta - \tfrac{1}{12}\rho u_0) y + \tfrac{1}{12}\rho u_0^2 y^2$$
$$f_7 = \tfrac{1}{6}\tau^2 \rho u_0^2 \delta^2 - \tfrac{1}{12}\tau \rho u_0^2 \delta^2 - \tfrac{1}{12}\tau \rho u_0 \delta + \tfrac{1}{36}\rho$$
$$+ (+\tfrac{1}{6}\tau \rho u_0^2 \delta + \tfrac{1}{12}\rho u_0) y + \tfrac{1}{12}\rho u_0^2 y^2$$
$$f_8 = \tfrac{1}{6}\tau^2 \rho u_0^2 \delta^2 - \tfrac{1}{12}\tau \rho u_0^2 \delta^2 + \tfrac{1}{12}\tau \rho u_0 \delta + \tfrac{1}{36}\rho$$
$$+ (+\tfrac{1}{6}\tau \rho u_0^2 \delta + \tfrac{1}{12}\rho u_0) y + \tfrac{1}{12}\rho u_0^2 y^2$$

For the Couette flow, the top boundary is a moving one; the analytical solution given here will give guidance in developing a suitable boundary condition for moving boundaries.

We note that these analytical solutions are valid for any u_0, τ, and δ. They will enhance our understanding of the method and will give guidance in applications.

ACKNOWLEDGMENTS

We should like to thank S. Chen, D. Noble, G. McNamara, D. d'Humières, D. Levermore, Y. H. Qian for helpful discussions. Q. Z. would like to thank the Associated Western Universities, Inc. for providing a faculty sabbatical fellowship and to thank S. Chen for helping to arrange for his visit to the Los Alamos National Lab.

REFERENCES

1. L. P. Kadanoff, G. R. McNamara, and G. Zanetti, A Poiseuille viscometer for lattice gas automata, *Complex Systems* **1**:791 (1987).
2. L. P. Kadanoff, G. R. McNamara, and G. Zanetti, From automata to fluid flow: Comparisons of simulation and theory, *Phys. Rev. A* **40**:4527 (1989).
3. M. Henon, Viscosity of a lattice gas, *Complex Systems* **1**:763 (1987).
4. R. Cornubert, D. d'Humières, and D. Levermore, A Knudsen layer theory for lattice gases, *Physica D* **47**(6):241 (1991).
5. L. S. Luo, H. Chen, S. Chen, G. D. Doolen, and Y. C. Lee, Generalized hydrodynamic transport in lattice-gas automata, *Phys. Rev. A* **43**:7097 (1991).
6. I. Ginzbourg and P. M. Adler, Boundary flow condition analysis for the three-dimensional lattice Boltzmann model, *J. Phys. II France* **4**:191 (1994).
7. D. R. Noble, S. Chen, J. G. Geogiadis, and R. O. Buckius, A consistent hydrodynamic boundary condition for the lattice Boltzmann method, *Phys. Fluids* **7**:203 (1995).
8. S. Chen, H. Chen, D. Martinez, and W. H. Matthaeus, Lattice Boltzmann model for simulation of magnetohydrodynamic phenomena, *Phys. Rev. Lett.* **67**:3776 (1991).
9. Y. Qian, D. d'Humières, and P. Lallemand, Lattice BGK models for Navier–Stokes equation, *Europhys. Lett.* **17**(6):479 (1992).
10. Y. H. Qian and S. A. Orszag, Lattice BGK models for the Navier–Stokes equation: Non-linear deviation in compressible regimes, *Europhys. Lett.* **21**(3):255 (1993).
11. S. Hou, Q. Zou, S. Chen, G. D. Doolen, and A. C. Cogley, Simulation of cavity flow by the lattice Boltzmann method, *J. Comput. Phys.* **118**:329 (1995).
12. D. P. Ziegler, Boundary conditions for lattice Boltzmann simulations, *J. Stat. Phys.* **71**:1171 (1993).
13. Y. H. Qian, Private communication.
14. P. A. Skordos, Initial and boundary conditions for the lattice Boltzmann method, *Phys. Rev. E* **48**:4823 (1993).
15. Y. Qian, Ph.D. thesis, Université Pierre et Marie Curie (January 1990).